

Characterisation of highly radiation-damaged SiPMs using current measurements

E. Garutti, R. Klanner*, D. Lomidze, J. Schwandt, and M. Zvolsky

*Institute for Experimental Physics, University of Hamburg,
Luruper Chaussee 147, D 22761, Hamburg, Germany.*

Abstract

The characterisation of radiation-damaged SiPMs is a major challenge, when the average time between dark counts approaches, or even exceeds, the signal decay time. In this note a collection of formulae is presented, which have been developed and used for the analysis of current measurements for SiPMs in the dark and illuminated by an LED, before and after hadron irradiation. It is shown, how parameters like the breakdown voltage, the quenching resistance, the dark-count rate, the reduction of the photo-detection efficiency due to dark counts and the Geiger discharge probability can be estimated from current-voltage measurements. The only additional SiPM parameters needed are the pixel capacitance, the number of pixels and the correlated noise. Central to the method is the concept of the pixel occupancy, the probability of a Geiger discharge in a single pixel during a given time interval, for which the decay time of the SiPM signal has been assumed. As an illustration the formulae are used to characterise a KETEK SiPM before and after irradiation by a fluence of $5 \times 10^{13} \text{ cm}^{-2}$ of reactor neutrons for temperatures of -30°C and $+20^\circ\text{C}$, where dark-count rates exceeding 10^{11} Hz are observed.

Keywords: SiPM, radiation damage, dark-count rate, photo-detection efficiency, pixel occupancy

Contents

1	Introduction	2
2	Model and formulae	2
2.1	Quenching resistance R_q	2
2.2	Rate of converting photons R_γ	2
2.3	Breakdown voltage V_{bd} , excess voltage V_{ex} , and gain G	3
2.4	Model for SiPM, pixel occupancy and photo-detection efficiency	3
2.5	Normalised SiPM currents with light	4
2.6	Dark-count rate DCR	5
3	Measurements and data analysis	5
3.1	Quenching resistance R_q	6
3.2	Breakdown voltage V_{bd}	6
3.3	Normalised SiPM currents with LED illumination	7
3.4	Pixel occupancy η , photo-detection efficiency and Geiger-discharge probability	9
3.5	Dark-count rate DCR	9
4	Summary and conclusions	10
5	List of References	10

*Corresponding author. Email address: Robert.Klanner@desy.de, Tel.: +49 40 8998 2558

1. Introduction

Radiation damage by hadrons is one of the major limitations for the use of silicon photomultipliers (SiPM) at high luminosity accelerators and in space research. Accordingly, the investigation of SiPM radiation damage and the improvement of their radiation hardness is a major research topic [1, 2, 3]. In this paper we develop methods to characterise SiPMs using current voltage measurements, which can also be applied at the high dark-count rates, DCR , where methods developed so far have difficulties. The data required are:

1. $I_{dark}(V_{for})$, the dark current measured for forward bias,
2. $I_{dark}(V_{rev})$, the dark current measured for reverse bias, and
3. $I_{dark+light}(V_{rev})$, the current measured with the SiPM illuminated by a DC light source.

From 2. and 3., we obtain the additional current from the illumination

$$I_{light} = I_{dark+light} - I_{dark}. \quad (1)$$

We note that for high DCR values, when the probability is significant that a dark count and a photon produce simultaneously an eh pair in the sensitive volume of the SiPM, I_{light} depends both on the light intensity and on the DCR.

For the analysis the following additional parameters, which cannot be obtained from current measurements, are required:

1. N_{pix} , the number of SiPM pixels,
2. C_{pix} , the single pixel capacitance,
3. C_q , the capacitance parallel to the quenching resistor, and
4. $1 + CN$, the increase in SiPM signal due to correlated noise.

The single pixel capacitance, C_{pix} and C_q have been obtained from the frequency dependency of the SiPM capacitance measured 0.5 V below the breakdown voltage at 20 °C divided by N_{pix} , [4]. For the formulae given, $C_q = 0$ is assumed. A finite value of C_q significantly complicates several of the formulae.

2. Model and formulae

2.1. Quenching resistance R_q

The quenching resistance, R_q , is obtained from $I_{dark}(V_{for})$ using

$$R_q = \left(\frac{dI_{dark}}{dV_{for}} \right)^{-1}. \quad (2)$$

It has been noticed that $R_q(V_{for})$ has a finite slope even at voltages as high as 2 V, and as noted in [4], the R_q value obtained from the frequency dependence of the capacitance 0.5 V below the breakdown voltage is more reliable.

2.2. Rate of converting photons R_γ

In this and in the following sections, we use V for the reverse voltage, V_{rev} . The rate of photons which generate eh pairs in the sensitive volume of the SiPM, R_γ , is estimated from I_{light} using

$$R_\gamma = \frac{I_{light}(V_{G=1})}{q_0}, \quad (3)$$

where a value of the reverse voltage $V_{G=1}$ has to be chosen, at which the SiPM gain $G = 1$. In the data analysis it should be checked that I_{light} is constant in the region of $V_{G=1}$.

We note that the assumptions that the R_γ does not change with V between $V_{G=1}$ and the SiPM operating voltage, is far from trivial. An increase in V increases the depletion region of the pn junction, which can increase the efficiency of an eh pair generated by light in the non-depleted region to reach the high electric-field region. In addition, radiation damage increases the silicon resistivity, and not all free charge carriers may be transported. However, as shown in Refs. [5, 6], this effect can probably be ignored for the high fields present in SiPMs.

2.3. Breakdown voltage V_{bd} , excess voltage V_{ex} , and gain G

For the determination of the breakdown voltage, V_{bd} , a method using the Inverse Logarithmic Derivative, $ILD = 1/(\frac{d \ln(I)}{dV})$ is recommended. A straight-forward way is to determine V_{bd} as the voltage at which ILD has its minimum [4, 7]. The minimum can be obtained by a parabolic interpolation using the three ILD values around the minimum. Another way is to fit the rising part of ILD with a first or second order polynomial and determine V_{bd} as the voltage at which the polynomial crosses the V axis. We found that the results are quite similar and use the *ILD-minimum method*. In the analysis it should be checked, that using I_{dark} , $I_{dark+light}$ and I_{light} give compatible results for V_{bd} .

The excess voltage is defined as

$$V_{ex} = V - V_{bd}. \quad (4)$$

Values $V_{ex} > 0$ correspond to the SiPM operating range as photo detector.

For the gain, G , the following, approximate relation is used

$$G = \frac{C_{pix} \cdot V_{ex}}{q_0}. \quad (5)$$

A more accurate relation is:

$$G = \frac{(C_{pix} + C_q) \cdot (V - V_{to})}{q_0}, \quad (6)$$

where C_q is an additional capacitance in parallel to R_q , and V_{to} the voltage at which the Geiger discharge *turns off*, as the current flowing through the pixel is too low to maintain a discharge. An additional capacitance C_q results in a fast initial pulse, which is implemented in SiPMs with larger pixels to improve the time resolution. As far as we know, there is no fundamental reason why $V_{to} = V_{bd}$. In [4] it has been shown that for the KETEK SiPM with a pixel size of $15 \mu\text{m}$ $V_{bd} - V_{to} \approx 1 \text{ V}$, whereas for similar KETEK SiPMs with pixel sizes of $25 \mu\text{m}$, $50 \mu\text{m}$ and $100 \mu\text{m}$, $V_{to} \approx V_{bd}$ has been found. In the following, we will make the assumption of Eq. 5 for G . Using the relation Eq. 6 instead of Eq. 5 is straight-forward; this however is not the case for a precise determination of C_q [7] and of V_{to} [4].

2.4. Model for SiPM, pixel occupancy and photo-detection efficiency

For the relation between the dark current, I_{dark} , and the dark-count rate, DCR , the Gain, G , and the correlated noise, CN , we assume

$$I_{dark}^{model} = q_0 \cdot DCR \cdot G \cdot (1 + CN) = q_0 \cdot G \cdot \frac{N_{pix} \cdot \eta_{DC}}{\Delta t}. \quad (7)$$

On the right-hand side, we have introduced the single-pixel occupancy, η_{DC} , which denotes the probability that a pixel, because of Dark Counts (DC s), is busy during the signal time Δt . The pixel occupancy includes the effects of the CN . From Eq. 7 we obtain $DCR \cdot (1 + CN) = N_{pix} \cdot \eta_{DC} / \Delta t$.

For the SiPM current with illumination in the presence of dark current, $I_{dark+light}$, we assume

$$I_{dark+light}^{model} = q_0 \cdot G \cdot \frac{N_{pix} \cdot \eta_{DC+light}}{\Delta t}, \quad (8)$$

where $\eta_{DC+light}$ is the single-pixel occupancy due to DC s and illumination.

For the SiPM current with illumination in the absence of a dark current, $I_{0\,dark+light}$, we assume

$$I_{0\,dark+light}^{model} = q_0 \cdot R_\gamma \cdot G \cdot (1 + CN) \cdot p_{Geiger} = q_0 \cdot G \cdot \frac{N_{pix} \cdot \eta_{light}}{\Delta t}, \quad (9)$$

where R_γ is the rate of photons producing eh pairs in the sensitive volume of the SiPM, and p_{Geiger} the probability of a photon to cause a Geiger discharge in the absence of pile-up due to the pixel occupancy by DC s.

In all 3 cases the relation between current and occupancy assumed is

$$I = \frac{q_0 \cdot N_{pix} \cdot G \cdot \eta}{\Delta t}. \quad (10)$$

Assuming

$$\Delta t = \tau \approx R_q \cdot C_{pix} \quad \text{and} \quad G = C_{pix} \cdot V_{ex}/q_0, \quad (11)$$

we obtain

$$\eta = \frac{I}{V_{ex}} \cdot \frac{R_q}{N_{pix}} = \frac{I}{I_{max}}, \quad (12)$$

where τ is the recharging time constant of the pixel, R_q the quenching resistance, and C_{pix} the pixel capacitance. The maximum current $I_{max} = N_{pix} \cdot V_{ex}/R_q$ corresponds to the situation for which the voltage drop over R_q is V_{ex} , i.e. a continuous Geiger discharge.

From η we estimate μ , the average number of eh pairs per time interval τ , which would produce Geiger discharges, if there were no pile-up effects

$$\mu = -\ln(1 - \eta). \quad (13)$$

This relation is valid if the number of Geiger discharges is distributed according to a Poisson distribution, but also for a Generalised Poisson distribution [8, 9], if the effect of the CN is included in η , as is the case here. However, the relation is only valid if all pixels behave the same, in particular have the same DCR . In Ref. [10] the DCR of individual pixels for non-irradiated KETEK SiPMs has been determined from the light produced by the Geiger discharges, and large pixel-to-pixel differences were observed. In Ref. [11] it is shown that these pixel-to-pixel differences even increase after irradiation with a fluence of 10^{10} thermal neutrons.

As the average number of eh pairs produced by DCS , μ_{DC} , and by the illumination, μ_{light} , is additive, we obtain for the average number of eh pairs from the illumination

$$\mu_{light} = \mu_{DC+light} - \mu_{DC}, \quad (14)$$

and for the multiplicative factor to the photon detection efficiency (pde), ε_{light} , which accounts for the reduction of the pde due to pixel occupancy

$$\varepsilon_{light} = \frac{\eta_{DC+light} - \eta_{DC}}{\mu_{light}} = \frac{\eta_{DC+light} - \eta_{DC}}{\ln\left(\frac{1 - \eta_{DC}}{1 - \eta_{DC+light}}\right)}. \quad (15)$$

The current increase due to the illumination, which can be compared to I_{light} defined in Eq. 1, is given by

$$I_{dark+light}^{model} - I_{dark}^{model} = I_{0dark+light}^{model} \cdot \varepsilon_{light} = q_0 \cdot G \cdot (1 + CN) \cdot R_\gamma \cdot p_{Geiger} \cdot \varepsilon_{light}. \quad (16)$$

As mentioned in Sect. 1, the additional current due to the illumination depends on R_γ as well as on the DCR . Eq. 16 can also be used to determine p_{Geiger} using only current measurements and an estimate of CN .

We note that for $(\eta_{DC+light} - \eta_{DC})/(1 - \eta_{DC}) \ll 1$, which corresponds to a low light intensity, the series expansion of Eq. 15 gives $\varepsilon_{light} \approx 1 - \eta_{DC}$. Thus the efficiency of the detection of photons is reduced by the probability that a Geiger discharge from a dark count already has occurred.

2.5. Normalised SiPM currents with light

A straight-forward method of obtaining an idea of the effects of radiation damage or temperature on the SiPM performance is to compare $I_{light}^{norm} = I_{light}/R_\gamma$ of a SiPM for different irradiation and measurement conditions [12, 13]. From Eq. 16 we obtain

$$\frac{I_{light}^{\Phi_2, T_2}/R_\gamma^{\Phi_2, T_2}}{I_{light}^{\Phi_1, T_1}/R_\gamma^{\Phi_1, T_1}} = \frac{G^{\Phi_2, T_2} \cdot (1 + CN^{\Phi_2, T_2}) \cdot p_{Geiger}^{\Phi_2, T_2} \cdot \varepsilon_{light}^{\Phi_2, T_2}}{G^{\Phi_1, T_1} \cdot (1 + CN^{\Phi_1, T_1}) \cdot p_{Geiger}^{\Phi_1, T_1} \cdot \varepsilon_{light}^{\Phi_1, T_1}}, \quad (17)$$

were the Φ_i denote the irradiation fluences and T_i the temperatures of two measurements. If V_{bd} is the only SiPM parameter which changes and the values of ε_{light} are the same, the I_{light}^{norm} ratio as function of excess voltage, will be 1. A deviation from 1 indicates a change of at least one of the SiPM parameters or of the occupancy. A systematic fluctuation of the ratio in the region of V_{bd} , where the shape of I_{light} varies rapidly, indicates a mismatch of the assumed V_{bd} values.

This method can be used to investigate the fluence dependence of the SiPM performance at a fixed temperature. For a non-irradiated SiPM with low DCR and illuminated well below saturation, $\varepsilon_{light} = 1$ can be assumed, and the I_{light}^{norm} ratio for the fluences Φ_1 to $\Phi_2 = 0$ as a function of V_{ex} will show, if the SiPM performance has changed. In a similar way the ratio, after taking into account the change of V_{bd} with temperature, can be used to investigate possible changes of the product $G \cdot (1 + CN) \cdot p_{Geiger} \cdot \varepsilon_{light}$ with temperature.

2.6. Dark-count rate DCR

Using Eqs. 7 and 11 one finds

$$DCR = \frac{N_{pix} \cdot \eta_{DC}}{R_q \cdot C_{pix}} \cdot \frac{1}{1 + CN} = \frac{I_{dark}}{C_{pix} \cdot V_{ex} \cdot (1 + CN)}, \quad (18)$$

which can be used to estimate the DCR . Another way of estimating the DCR for high fluences is to assume that G and CN , after taking into account a possible change of V_{bd} , do not depend on fluence. Then the DCR scales with I_{dark} , and, if the DCR at a low fluence Φ_1 is known, the approximate DCR at a high fluence Φ_2 is given by:

$$DCR_{\Phi_2} = \frac{I_{dark}^{\Phi_2}}{I_{dark}^{\Phi_1}} \cdot DCR_{\Phi_1}. \quad (19)$$

This relation is useful, if the DCR at a low fluence Φ_1 has been determined from the pulse height spectrum measured in the dark. However, the assumption that G and CN are the same for both conditions has to be checked, which can be done using the ratio of normalised currents with illumination discussed in Sect. 2.5, or C_{pix} determinations using capacitance–frequency measurements at voltages close to V_{bd} [7].

3. Measurements and data analysis

In this section we use some of the formulae presented in Sect. 2 to characterise a KETEK SiPM with a $15 \mu\text{m}$ pixel size before and after irradiation by reactor neutrons with a dose of $5 \times 10^{13} \text{ cm}^{-2}$. The number of pixels $N_{pix} = 4384$, and in [4] $C_{pix} = 18 \text{ fF}$ and $C_q < 5 \text{ fF}$ have been determined with capacitance–frequency measurements 0.5 V below V_{bd} at 20°C [4]. The following current measurements, taken at -30°C and $+20^\circ\text{C}$

1. $I_{dark}(V_{for})$, the dark current measured for forward bias between 0 and 2 V,
2. $I_{dark}(V_{rev})$, the dark current measured for reverse bias, between 0 and 35 V, and
3. $I_{dark+light}(V_{rev})$, the current measured with the SiPM illuminated by a blue LED, between 0 and 40 V.

were analysed. For 3., measurements at two different LED light intensities, "low LED" and "high LED", were made. To check the quality of the measurements, the voltage was ramped up and down for V_{for} and V_{rev} , and it was checked if the results agree. With the exception of the measurements at -30°C and low LED, the agreement was within 1%. For the -30°C data, discrepancies at the 30% level were observed. Unfortunately the measurements could not be repeated, as this SiPM stopped working. We note that we do not have a complete data set for the same SiPM before and after irradiation, and the measurements for the non-irradiated and irradiated SiPM come from different samples. As a result, some of the differences of the SiPM parameters before and after irradiation, in particular the values of R_q and V_{bd} , are ascribed to the different SiPMs.

3.1. Quenching resistance R_q

The quenching resistance, R_q , was determined from I_{dark} measured at V_{for} at 1.6 and 1.8 V using Eq. 2. We could not use the data at 2 V, because the current exceeded the current limit of voltage source for some measurements. The results are presented in Table 1. We ascribe most of the increase of R_q with fluence to irradiation effects: Measurements at $+20^\circ\text{C}$ of the same SiPM before and after irradiation show an increase of R_q by $\approx 40\%$ after a fluence of $\Phi = 5 \times 10^{13} \text{ cm}^{-2}$. In addition, sample to sample differences of up to $\pm 30\%$ have been observed. A decrease of R_q with temperature is expected for a poly-Si resistor, due to increase of the intrinsic charge-carrier concentration. For the ratio $R_q(-30^\circ\text{C})/R_q(+20^\circ\text{C})$ a value of 0.645 is observed for both non-irradiated and irradiated SiPM. We also note that the values of R_q determined using $C - V$ measurements $\approx 0.5 \text{ V}$ below V_{bd} [4], are about 10% lower than the ones obtained from $I - V_{for}$. As the value of R_q obtained from the $I - V_{for}$ measurements depends on the choice of the V_{for} interval, we consider the $C - V$ results to be more accurate.

$T [^\circ\text{C}]$	$R_q [\text{k}\Omega]$	$R_q [\text{k}\Omega]$	$\frac{R_q(0)}{R_q(5 \times 10^{13})}$	$V_{bd} [\text{V}]$	$V_{bd} [\text{V}]$
	$\Phi = 0 \text{ cm}^{-2}$	$\Phi = 5 \times 10^{13} \text{ cm}^{-2}$		$\Phi = 0 \text{ cm}^{-2}$	$\Phi = 5 \times 10^{13} \text{ cm}^{-2}$
-30	811 ± 40	1313 ± 65	1.61 ± 0.11	26.298 ± 0.010	26.450 ± 0.010
+20	519 ± 26	849 ± 43	1.63 ± 0.13	27.391 ± 0.010	27.557 ± 0.010

Table 1: Values of R_q and V_{bd} from the $I - V$ measurements. The errors given present the uncertainties of the data and analysis, but do not include systematics. The measurements for the non-irradiated and irradiated SiPM were made on different samples. The differences for the two dose values in R_q are ascribed mainly to the irradiation, and the ones in V_{bd} to differences between the two SiPM samples and not to irradiation effects.

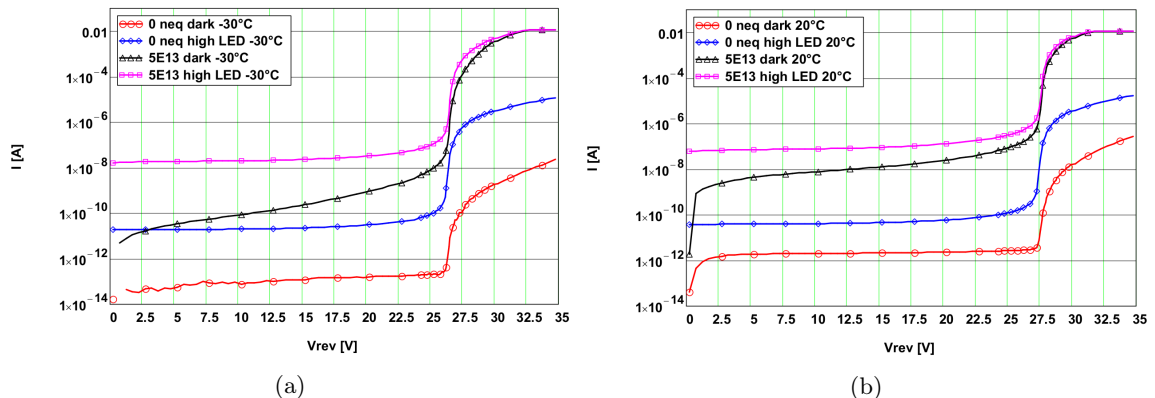


Figure 1: Comparison of the $I - V_{rev}$ measurements before and after neutron irradiation to $5 \times 10^{13} \text{ cm}^{-2}$ with and without LED illumination at (a) -30°C , and (b) $+20^\circ\text{C}$. The current limit of the voltage source is set to 12 mA, which causes the current saturation at high voltages.

3.2. Breakdown voltage V_{bd}

Fig. 1 shows the $I - V_{rev}$ data. Below $V_{bd} \approx 27 \text{ V}$, the dark current, I_{dark} , for the non-irradiated SiPM is approximately constant and hardly shows an increase due to avalanche multiplication, when approaching V_{bd} . We conclude that for the non-irradiated sensor most of the I_{dark} misses the amplification region and is not generated in the sensitive region of the SiPM. After irradiation, I_{dark} increases by 3 – 4 orders of magnitude, and a continuous increase of I_{dark} with voltage as well as avalanche multiplication are observed, which indicates that most of I_{dark} is generated in the sensitive region of the SiPM. Above the V_{bd} and below the current limit of the voltage source of 12 mA, I_{dark} increases by about 6 orders of magnitude due to the irradiation, but the shapes of the $I - V$ curves for the non-irradiated and irradiated SiPM are similar.

The voltage dependencies of the currents with LED irradiation, $I_{dark+light}$, are very similar and appear to depend neither on irradiation fluence nor on temperature. $I_{dark+light}$ is essentially

constant at low voltages, shows an increase due to avalanche multiplication when approaching V_{bd} , and, when passing and exceeding V_{bd} , the expected rapid increase due to Geiger discharges.

From the $I - V$ data the breakdown voltage, V_{bd} has been determined using the *minimum ILD* method discussed in Sect. 2.3. Fig. 2 shows the *ILD* curves and Table 1 the V_{bd} values. The *ILD* curves from I_{dark} of the non-irradiated SiPM are not shown, as I_{dark} of the non-irradiated SiPM is low, resulting in big *ILD* fluctuations.

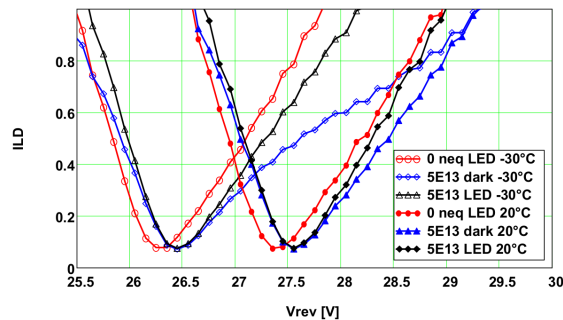


Figure 2: Inverse Logarithmic Derivative, *ILD*, for the $I - V$ data shown in Fig. 1.

The values of V_{bd} obtained from I_{dark} and $I_{dark+light}$ agree within their uncertainties. For the two temperatures, within the experimental uncertainties, the same difference (152 ± 14 mV at -30°C and 166 ± 14 mV at $+20^\circ\text{C}$) for the V_{bd} values for the non-irradiated and irradiated SiPM is observed. We ascribe this difference to the different SiPM samples investigated. In Ref. [13], using measurements at $+20^\circ\text{C}$ it is shown that for the KETEK SiPM investigated, V_{bd} does not change with irradiation up to a fluence of $5 \times 10^{13} \text{ cm}^{-2}$. For both, the non-irradiated and the irradiated SiPM, the temperature dependence of V_{bd} is $22.0 \text{ mV}/^\circ\text{C}$.

3.3. Normalised SiPM currents with LED illumination

From the measured currents with and without LED illumination, I_{light} is determined using Eq. 1, and with the help of Eq. 3, R_γ , the rate of photons generating eh pairs in the sensitive region of the SiPM. The results for R_γ are shown in Table 2. For $V_{G=1} = 10$ V has been chosen. Taking values of 5 V or 15 V changes the R_γ values by less than 5%.

T [$^\circ\text{C}$]	R_γ low LED [s^{-1}] $\Phi = 0 \text{ cm}^{-2}$	R_γ high LED [s^{-1}] $\Phi = 0 \text{ cm}^{-2}$	R_γ low LED [s^{-1}] $\Phi = 5 \times 10^{13} \text{ cm}^{-2}$	R_γ high LED [s^{-1}] $\Phi = 5 \times 10^{13} \text{ cm}^{-2}$
-30	6.2×10^7	12.5×10^7	6.9×10^{10}	20.3×10^{10}
+20	12.5×10^7	24.8×10^7	12.5×10^{10}	44.5×10^{10}

Table 2: Values of R_γ from the $I_{light} - V$ data using Eq. 3 with $V_{G=1} = 10$ V.

Fig. 3 shows the normalised current with illumination, $I_{light}^{norm} = I_{light}/(q_0 \cdot R_\gamma)$ as a function of V_{ex} . Up to $V_{ex} \approx 0.5$ V, I_{light}^{norm} neither depends on temperature nor on fluence, and we conclude, as discussed in Sect. 2.5, that in this voltage range the SiPM performance is the same for the different measurement conditions. At ≈ 0.5 V the $\Phi = 5 \times 10^{13} \text{ cm}^{-2}$, $T = 20^\circ\text{C}$, and at ≈ 2 V the $\Phi = 5 \times 10^{13} \text{ cm}^{-2}$, $T = -30^\circ\text{C}$ curves start to deviate from the $\Phi = 0$ results, and become constant at 2.5 V and 3.5 V, respectively. At these voltages the SiPM is no more a useful photo-detector, as the gain G , which is proportional to V_{ex} , is compensated by the loss in detection efficiency. For the $\Phi = 0$ data, the dependence of I_{light}^{norm} on V_{ex} is approximately independent of temperature and light intensity.

Fig. 4 a) shows the ratios of the normalised currents with illumination, defined in Eq. 17, for $\Phi_2 = 5 \times 10^{13} \text{ cm}^{-2}$ to $\Phi_1 = 0$ as a function of V_{ex} of the -30°C and of $+20^\circ\text{C}$ data for the low and the high LED intensity. As the V_{bd} values are different for the Φ_1 and the Φ_2 data, a cubic spline interpolation has been used to calculate the values of I_{light}^{norm} at the voltages of the Φ_1 measurements. Per definition, the ratio at $V_{ex} \approx -17$ V, which corresponds to $V_{rev} = V_{G=1} = 10$ V, is 1. The

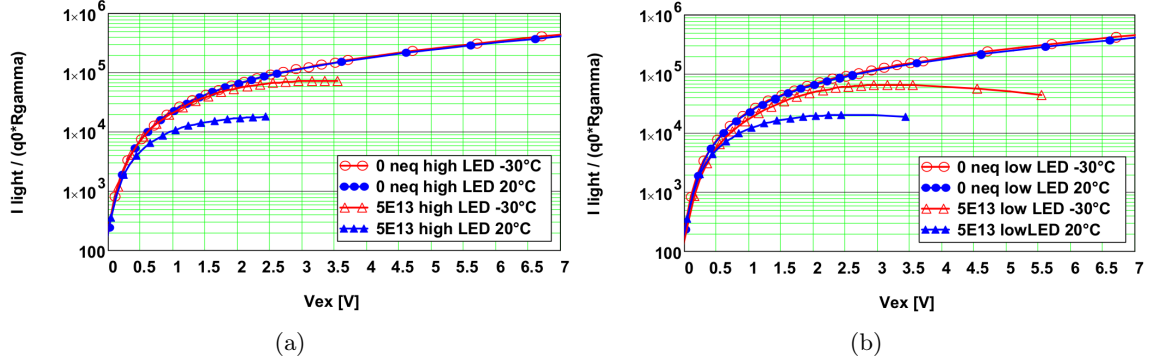


Figure 3: Normalised I_{light} as function of V_{ex} for (a) "high LED", and (b) "low LED". According to Eq. 16, $I_{light}/(q_0 \cdot R_\gamma) = G \cdot (1 + CN) \cdot p_{Geiger} \cdot \varepsilon_{light}$.

ratio rises up to ≈ 1.1 at the breakdown voltage, $V_{ex} = 0$, and then drops to zero due to the reduction of the photo-detection efficiency. The rise for $V_{ex} < 0$ may be evidence for differences in the increase of the multiplication gain with voltage below V_{bd} . As will be shown in Sect. 3.4, the main reason for the decrease for $V_{ex} > 0$ is the increase in pixel occupancy by dark counts and photons. As expected from the pixel occupancy, the decrease at $+20^\circ\text{C}$ is faster than at -30°C , and also faster for the high than for the low LED intensity. We note a difference in shape of the -30°C low LED curve compared to the other 3 curves, which we ascribe to the measurement problem discussed at the beginning of Sect. 3.

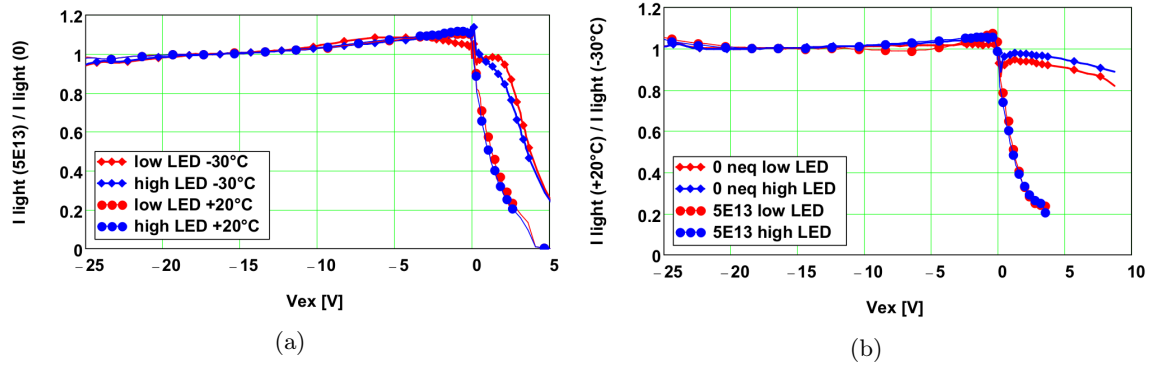


Figure 4: Normalised current ratio with illumination (Eq. 17) as a function of V_{ex} . (a) $(I_{light}^{5 \times 10^{13}, T} / R_\gamma^{5 \times 10^{13}, T}) / (I_{light}^{0, T} / R_\gamma^{0, T})$ at $T = -30^\circ\text{C}$ and $+20^\circ\text{C}$, and (b) $(I_{light}^{\Phi, +20^\circ\text{C}} / R_\gamma^{\Phi, +20^\circ\text{C}}) / (I_{light}^{\Phi, -30^\circ\text{C}} / R_\gamma^{\Phi, -30^\circ\text{C}})$ at $\Phi = 0$ and $5 \times 10^{13} \text{ cm}^{-2}$.

Fig. 4b) shows the ratios of the normalised currents with illumination for $T_2 = +20^\circ\text{C}$ to $T_1 = -30^\circ\text{C}$ at $\Phi = 0$ and $5 \times 10^{13} \text{ cm}^{-2}$ for the low and high LED intensities. For the non-irradiated SiPM we note a shift of the ratio by about $+3\%$ between the high- and low-LED data for voltages around and above $V_{ex} = 0$, which we do not understand and which may indicate a measurement problem. At $V_{ex} = 0$ the ratios drop by $\approx 7\%$, with a further decrease by about the same amount up to $V_{ex} = 8 \text{ V}$, the maximum value of the measurements. The results suggest that the value of $p_{Geiger} \cdot (1 + CN)$ decreases with increasing temperature. However, further studies, in particular a comparison to pulse-height measurements as a function of temperature, are required to verify this conclusion.

For the irradiated SiPM the current ratio drops from 1 to ≈ 0.2 between $V_{ex} = 0$ and 3 V , where the measurements at $+20^\circ\text{C}$ reach the current limit. As will be shown in Sect. 3.4 this rapid decrease of the ratio is due to the increase of DCR between 30°C and $+20^\circ\text{C}$.

3.4. Pixel occupancy η , photo-detection efficiency and Geiger-discharge probability

Fig. 5 shows the pixel occupancies, η_{DC} , $\eta_{DC+lowLED}$ and $\eta_{DC+highLED}$ calculated using Eq. 12. For the non-irradiated SiPM (Fig. 5 a), the η values are well below 10^{-3} for all measurement conditions, and no significant reduction of the pde due to the occupancy is expected. For the SiPM irradiated to $5 \times 10^{13} \text{ cm}^{-2}$ (Fig. 5 b), the η values increase rapidly with V_{ex} reaching values close to 60%, and we expect a significant decrease in pde , as photons hitting a pixel in coincidence with a Geiger discharge from a dark count, will produce no or reduced signals. As expected, $\eta_{DC+highLED} > \eta_{DC+lowLED} > \eta_{DC}$, and the increase of η due to photons has to be taken into account in the analysis.

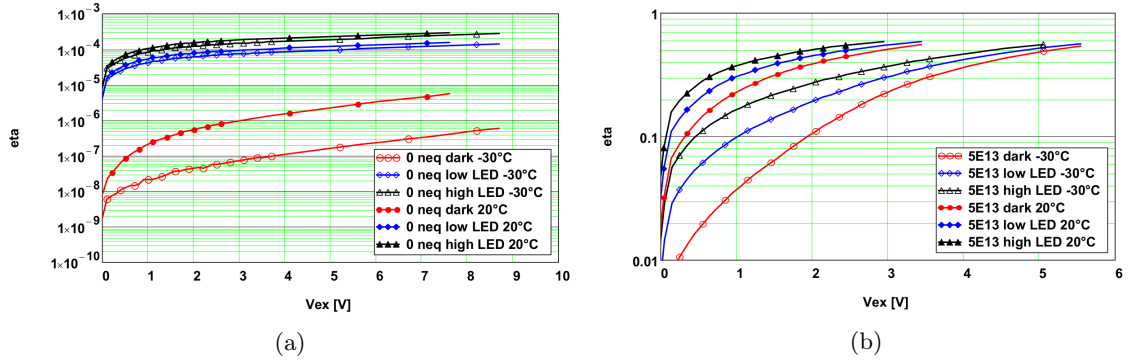


Figure 5: Pixel occupancies, η calculated using Eq. 12 for (a) the non-irradiated, and (b) the SiPM irradiated to $5 \times 10^{13} \text{ cm}^{-2}$.

Fig. 6 shows the product $p_{Geiger} \cdot (1 + CN)$ calculated using Eq. 16 as a function of V_{ex} . For the non-irradiated SiPM the curve rises quickly above V_{bd} , and after some flattening continues to rise at higher values of V_{ex} . The rise for -30°C is faster than for 20°C . Based on the results of Ref. [9], we ascribe this rise to the increase of correlated noise, CN , with V_{ex} . The $\Phi = 5 \times 10^{13} \text{ cm}^{-2}$ data follow the curves of the non-irradiated SiPM up to $\approx 0.75 \text{ V}$ for the 20°C data, and up to $\approx 2.5 \text{ V}$ for the -30°C data, and after reaching a maximum, decrease. We assume that this decrease is due to the high occupancy of the individual pixels: The pixels do not reach anymore the full biasing voltage.

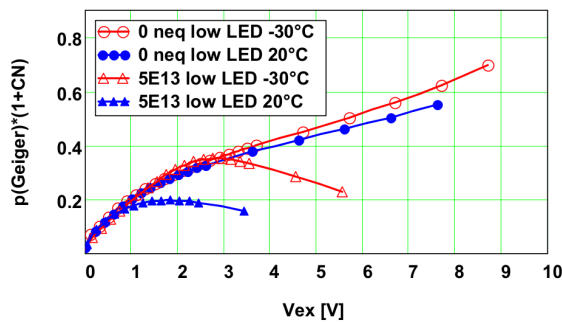


Figure 6: Product $p_{Geiger} \cdot (1 + CN)$, calculated using Eq. 16, as a function of V_{ex} .

3.5. Dark-count rate DCR

Fig. 7 shows the product $DCR \cdot (1 + CN)$ calculated using Eq. 18 as a function of V_{ex} . As reported in Ref. [9], typical values of CN at 20°C for the KETEK SiPM investigated are 0.05 at $V_{ex} = 3.5 \text{ V}$ and 0.20 at 7.5 V . It can be seen that the DCR increases by approximately an order of magnitude between -30°C and $+20^\circ\text{C}$, and by about six orders of magnitude between no irradiation and irradiation to $5 \times 10^{13} \text{ cm}^{-2}$. The value $DCR = 10^{11} \text{ Hz}$ corresponds to 10 000 dark

counts for a 100 ns gate, which is typically used for pulse-height measurements. Thus, deriving the DCR from pulse-height spectra under these conditions is difficult, if not impossible.

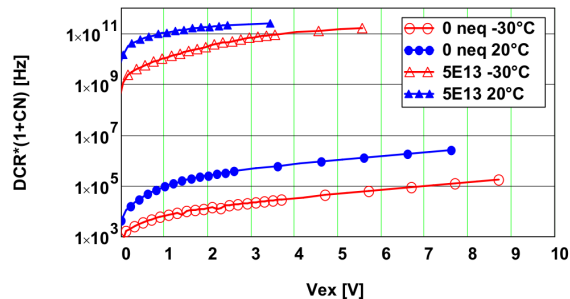


Figure 7: Product $DCR \cdot (1 + CN)$, calculated using Eq. 18, as a function of V_{ex} .

4. Summary and conclusions

In this note a fairly complete set of formulae is derived, which allows characterising SiPMs before and after irradiation with hadrons using current-voltage measurements with and without illumination. Central to the proposed method is the concept of the pixel occupancy, η , the probability that a pixel is *busy* or *occupied* by a Geiger discharge during a time interval Δt , from which the loss in photo-detection efficiency due to pile-up can be estimated. For Δt the recharging time of a pixel $\tau = R_q \cdot C_{pix}$ is assumed. The SiPM parameters determined with the proposed method are the quenching resistance, R_q , the breakdown voltage, V_{bd} , the pixel occupancy, η , the products of correlated noise times Geiger discharge probability, $(1 + CN) \cdot p_{Geiger}$, and dark-count rate, $(1 + CN) \cdot DCR$. The formulae allow to extend the characterisation of SiPMs into the region of $DCRs$ well above 10^{10} Hz, where other methods, like the analysis of pulse height spectra or transient current measurements, are having difficulties. Although the derivation of the formulae is straight-forward, the understanding of the validity of the assumptions made is much less obvious.

To illustrate the application of the formulae and to investigate their validity, they are used to analyse current-voltage characteristics of a KETEK SiPM with $15 \mu\text{m}$ pixel size, measured with and without illumination by light from an LED at temperatures of -30°C and $+20^\circ\text{C}$, before and after neutron irradiation to a fluence of $5 \times 10^{13} \text{ cm}^{-2}$, where dark-count rates exceeding 10^{11} Hz are observed.

Further applications of the formulae for the analysis of SiPM data will show to which extent they are valid, and which of the proposed methods are of practical use. The reader is strongly encouraged to try the formulae for the analysis of his SiPM measurements, and communicate failures and successes. This will help to improve the method. In addition, an attempt is made to clearly define all technical terms used. It is hoped that this will help to find a common nomenclature for the characterisation of SiPMs – photo detectors with a most promising future.

5. List of References

References

- [1] Y. Musienko et al., *Study of radiation damage induced by 82 MeV protons on multi-pixel Geiger-mode avalanche photodiodes*, Nuclear Instruments and Methods in Physics Research A610 (2009) 87–92, doi.org/10.1016/j.nima.2009.05.052.
- [2] Yi Quiang et al., *Radiation hardness tests of SiPMs for the JLab Hall D Barrel calorimeter*, Nuclear Instruments and Methods in Physics Research A698 (2013) 243–241, doi.org/10.1016/j.nima.2012.10.015.

- [3] A. Heering et al., *Effects of very high radiation on SiPMs*, Nuclear Instruments and Methods in Physics Research A824 (2016) 111–114, doi.org/10.1016/j.nima.2015.11.037.
- [4] V. Chmill, et al., *Study of the breakdown voltage of SiPMs*, Nuclear Instruments and Methods in Physics Research Section A845 (2017) 56–59, doi.org/10.1016/j.nima.2016.04.047.
- [5] B. Wiederspan, *Investigation of the influence of the photo current on the charge density of radiation damaged silicon pad diodes*, BSc thesis, University of Hamburg, Sept. 2017, unpublished.
- [6] Ch. Scharf, *Development of a radiation-tolerant pixel sensor for the HL-LHC*, PhD thesis, University of Hamburg, Oct. 2017, to be published as DESY Thesis.
- [7] Ch. Xu et al., *Influence of X-ray irradiation on the properties of the Hamamatsu silicon photomultiplier S10362-11-050C*, Nuclear Instruments and Methods in Physics Research Section A762 (2014) 149–161, doi.org/10.1016/j.nima.2014.05.112.
- [8] S. Vinogradov, *Analytical models of probability distribution and excess noise factor of solid state photomultiplier signals with crosstalk*, Nuclear Instruments and Methods in Physics Research Section A695 (2012) 247–251, doi.org/10.1016/j.nima.2011.11.086.
- [9] V. Chmill, et al., *On the characterisation of SiPMs from pulse-height spectra*, Nuclear Instruments and Methods in Physics Research Section A854 (2017) 70–81 doi.org/10.1016/j.nima.2017.02.049.
- [10] E. Engelmann et al., *Impact of Local Defects on the Dark Count Rate of SiPM*, Contribution to Session N18-4 of the 2016 IEEE Symposium on Nuclear Science, Strasbourg, 2016.
- [11] E. Engelmann et al., *Investigation of Radiation Hardness of SiPM Using the Effect of Hot Carrier Luminescence*, Contribution to the 2017 NDIP Conference, submitted for publication in Nuclear Instruments and Methods in Physics Research Section A.
- [12] M. Centis Vignali et al., *Neutron induced radiation damage of KETEK SiPMs*, Contribution to the 2016 IEEE Symposium on Nuclear Science, Strasbourg, 2016.
- [13] M. Centis Vignali et al., *Neutron irradiation effect on SiPMs up to $\Phi_{neq} = 5 \times 10^{14} \text{ cm}^{-2}$* , Contribution to the 2017 NDIP Conference, arXiv 1709.04648, submitted for publication in Nuclear Instruments and Methods in Physics Research Section A.